Mindanao Journal of Science and Technology Vol. 17 (2019) 195-213

Utilization of River Depth Profile and Historical Transects for the Estimation of Sedimentation and Flood Simulation

Edgar Allan C. Po[1*], Mark Alexis O. Sabines[2] and Jan Taat[3]
[1]College of Agriculture
University of Science and Technology of Southern Philippines – Claveria
Claveria, 9004 Philippines
[*]*poea@ustp.edu.ph*

[2]College of Agriculture
[3]College of Engineering
Xavier University – Ateneo de Cagayan
Cagayan de Oro City, 9000 Philippines

Date received: October 1, 2018
Revision accepted: January 25, 2019

Abstract

Bathymetric data is needed to properly manage river systems. However, bathymetric data generation needs specialized equipment, which may not always be available. Also, the ease of deployment and cost prevent its use on a regular, short to medium term basis. This study demonstrated a set of methodology that generated bathymetric data utilizing a raft and associated equipment setup. The observed mean depth of the river was 2.92 m (standard deviation: 0.84 m, n = 1981; range: 0.21 - 14.51 m). An estimation of the number of sediments lost and gained for a particular section of the river indicated a net loss of 0.48 m^3m^{-2}. A flood simulation on a subsection of the river caused by a 2-, 4- and 6-meter water level increase resulted in 164, 211 and 245 hectares of flooded zones, respectively.

***Keywords**:* echo sounders, GPS, sediment load, river depth, sediment loss, bathymetric

---

1. Introduction

The continuing threat of global warming, as manifested in the occurrence of stronger typhoons and hurricanes worldwide (Oouchi *et al.*, 2006), necessitates a review of available datasets that can be tapped and analyzed to help provide solutions to impacts of storms. On the micro level, a manifestation of the negative impact of increased typhoons and hurricanes can be seen in flood incidences. However, the necessary river dataset for the formulation of a scientifically-based mitigation plan is not available in many developing countries like the Philippines. A scientifically based mitigation plan is useful to land managers and emergency response teams by providing an understanding of flow hydraulics, flood routing, sediment transport, aquatic habitat, and the monitoring of geomorphic change. All of which are dependent on the quality of the three-dimensional (3D) representation of a river system (Hilldale and Raff, 2008; Trigg *et al*., 2009; Alfieri *et al*., 2016; Perez *et al*., 2016; Grimaldi *et al*., 2018). Despite its importance, bathymetric data is inadequate, if not absent, for many river systems in the world that are prone to flooding (Hilldale and Raff, 2008; Garcıa-Pintado *et al*., 2015; Wood *et al*., 2016). To further complicate things, a river geometry is not static, as the occurrence of flood events necessarily leads to its alteration (Buffington, 2012; Soar *et al*., 2017). Hence, there is a need for a regularly updated bathymetric information and data on river systems.

The Cagayan de Oro River in Northern Mindanao in the southern part of the Philippines had a flood event caused by tropical storm Sendong (internationally named "Washi") in 2011. The catastrophic flood caught the population living along its banks by surprise, resulting to a death toll of 1,472. The Cagayan de Oro river basin serves as a conduit of waters coming from the upland watershed areas of neighboring Bukidnon Province to the seas. A 180 mm rain event within the Cagayan de Oro area, coupled with discharges from the areas of Bukidnon, overwhelmed the river system, resulting in a large swath of area covered by flood waters that were not accommodated by the river channel (Manila Observatory, 2011). In a short temporal/time range, the flood water rose from its normal level to almost 5 m, and even higher, in some areas. A visual examination of river banks affected by the flood revealed soil particles literally transported downstream by the fast-moving flood waters, leaving exposed sand, gravel, and boulders. There were a number of landslides that occurred upstream which could have substantially contributed to the sediment load carried at the height of the storm. The calamity highlights the lack or absence of basic data to create a proactive flood mitigation plan. Before any strategy can be crafted to mitigate the impact of flooding, there is a need to quantify its effects on the morphological structure of the river in terms of water level depth (Lane *et al*., 1994). The results provided primary data to either be improved with extensive follow-up studies or serve as a starting point for informed planning, decision making and formulation of policies for a responsible river dredging and flood mitigation program.

This study was conducted to generate baseline information on the bathymetric structure of the Cagayan de Oro River using mapping grade Global Positioning System receiver (GPSr) and echo-sounder, since there was no existing data at that time on a river that was prone to flooding. The use of

GPSr and echo-sounder (sonar sensor) provided an opportunity to generate bathymetric dataset that can be useful for the responsible management of the Cagayan de Oro River. The objectives of the study included a) designing a raft platform for river depth profiling equipped with an echo sounder and a mapping-grade GPSr; b) creating a 3D bathymetric model of the Cagayan de Oro River; c) acquiring and processing secondary data, and coming up with sample estimates of the net lost and gained sediments of the river system; and d) running a simulation on a sub-section of the river to quantify how increases in water level determine the extent of flooding on communities living near the river banks.

2. Methodology

2.1 Study Area

The river depth profiling was conducted along a segment of the Cagayan de Oro River from Bubunawan junction (124° 37.36’, 8° 24.0’) to near the river delta at Barangay Bonbon (124° 39.40’, 8° 30.34’), with a distance of 16.8 and 22 kilometers for the first and second day of the survey, respectively (Figure 1).

All the waters draining out from the Cagayan de Oro watershed (136,046.82 hectares) (DENR, 2017) goes through this river. The survey team was composed of two guide or rowers; person in-charge of documentation using both a video and a still camera; a GPSr equipment handler; an echo sounder device operation in-charge; and an overall support staff, bringing the total to six during the first day. There was a reorganization of roles on the second day with only five team members.

2.2 Survey Instrumentation, Physical Setup and Data Collection

The raft platform designed for the study consisted of a Zetec river raft (model 450R [SB]; Zetec Corp., Snoqualmie, WA) fitted with a marine ply-board platform placed across the middle of the raft to accommodate placement of the monitoring screen of the sonar sensor used in the project. Figure 2 shows a graphic illustration of the setup used in the study.

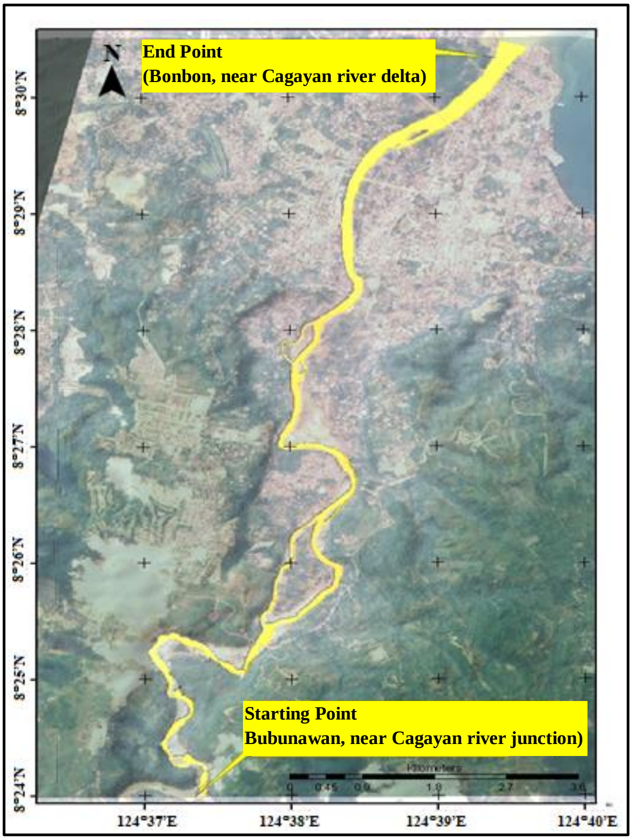

Figure 1. River depth profile study coverage

A sonar sensor Humminbird 581i (Johnson Outdoors, Eufaula, AL) was used in the study. Similar recreational-use sonar sensors from Humminbird were used in other bathymetric studies (Shcherbina *et al.*, 2008; Ceylan and Ekizoglu, 2014; Drakopoulou *et al*., 2018). Visual documentation of the survey was obtained using a digital video recorder. A mapping-grade GPSr, Trimble ProXRS (Trimble Navigation Ltd., Sunnyvale, California, USA) capable of obtaining positional data at sub-meter accuracy, was used in the survey as a roving unit to collect elevation data on the river surface.

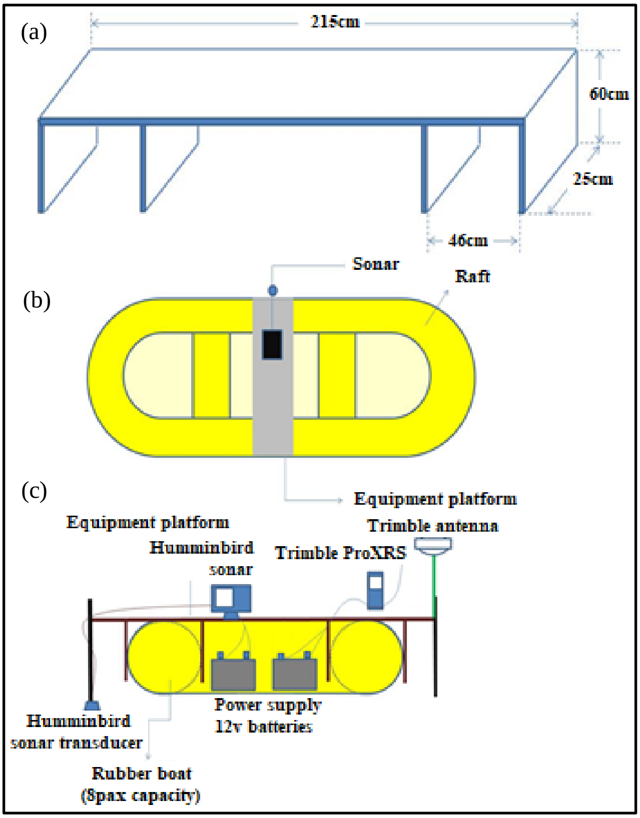

Figure 2. Representation of raft platform used in the bathymetric survey showing survey instruments support structure (a), placement of structure on the raft (b), and placement of equipment (c).

A significant limitation of the methodology used in this study was that in autonomous mode (i.e., without any correction), the Trimble ProXRS GPSr has a 100 m accuracy from true ground location as per specifications. Fortunately, after the GPSr was manufactured, the United States government decided to turn off selective availability (the one causing the 100m accuracy), and the Global Positioning System (GPS) precision has improved significantly to a global average user range error (URE) of ≤7.8 m (25.6 ft.), with 95% probability (US Department of Defense, 2008). The URE was still large for purposes of this study and there was a need to calibrate readings obtained by the study. To achieve the centimeter level positional accuracy, calibration protocol was implemented by setting up a temporary base station. Two GPSr units were used, with one (base station) placed over a survey monument (whose coordinates/location was known through calibration in the context of the Philippine national grid system) established by the Land Management Bureau of the Department of Environment and Natural Resources (DENR) of the Philippine government, and another one (rover) placed where the temporary base station was to be located some 2.9 km to the northwest. Both GPSr units collected locational data for three hours. After which, the data collected was used to perform post processing where the location of the rover can be within 1 cm from its true position. This increased accuracy was made possible as the two GPSr units used signals from the same satellites in space. The base station had a known location, and any deviation in the reading was interpreted as error. The amount of error in the base station was removed from the rover location readings by a process known as differential correction which was done through a proprietary post-processing software Trimble GPS Pathfinder Office v2.9. On the day of the survey and on the previously noted marker of the rover, a GPSr was placed (now serving as temporary base station) and recorded positional data for the entire duration of the survey. When the survey was over, data from the rover used in traversing the river was differentially corrected. There was no real time correction done on locational data taken by the rover placed on the raft. Error in location due to GPS signal bouncing off trees and other objects before reaching the antenna (known as multipath) of the GPSr were determined by the software and not included in the differential correction. The position of the raft was based on the post-processed differentially corrected location. The readings from the sonar were assigned to the corresponding location based on time stamp of the data.

2.3 River Bed Morphology/Bathymetry and Topographic Data

Figure 3 outlines the cartographic model followed by the study to generate the necessary 3D depth profile of the Cagayan de Oro River. Logged data from the sonar unit was imported to ArcGIS 9.2 (ESRI, Redlands, CA), a Geographic Information System (GIS) software, and converted to shapefile format. All data processing undergone by this study utilized the Universal Transverse Mercator (UTM), Zone 51N projection.

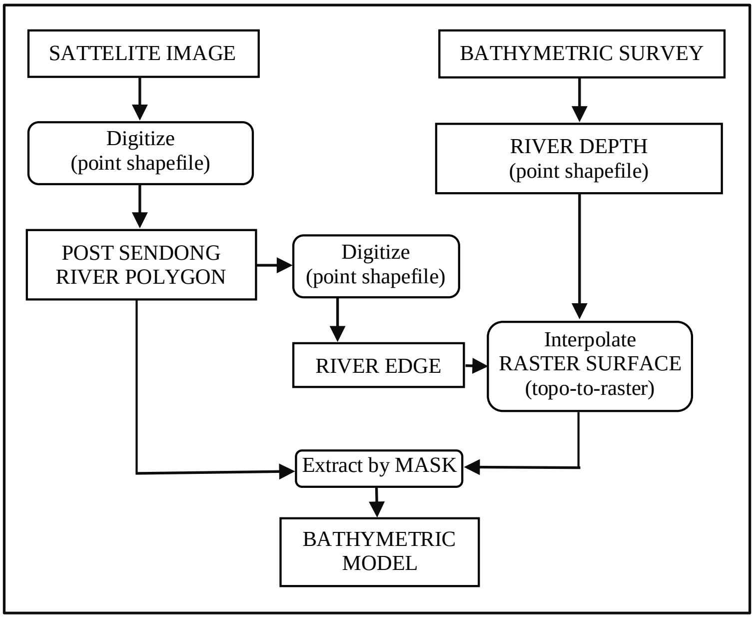

Figure 3. Cartographic model followed within ArcGIS 9.2 software environment to generate a 3D river depth profile of the Cagayan de Oro River

To be able to generate a 3D representation of river depth delineating the location of the river from the surrounding landscape, a JAXA (Japan Aerospace Exploration Agency) Advanced Land Observing Satellite (ALOS) satellite image with 2 m spatial resolution and a position accuracy of 1 m was downloaded. The area of the river was digitized and stored as polygon shapefile covering the entire survey stretch (approximate area = 196 hectares or 1.96 square kilometers) by tracing the visible river edge. Points at the edges were digitized (n = 4484) and given a zero depth to serve as the boundary of the river during the interpolation process.

The Humminbird had a total of 1981 sonar readings of which 1721 were used to generate the river bathymetric model. The remaining 269 data points were set aside as validation dataset (Traganos *et al*., 2018). The Topo-to-Raster tool of ArcGIS 9.2 was employed to interpolate the depth surface because of its capability to generate hydrologically-correct digital elevation model using an interactive finite difference interpolation technique (Hutchinson, 1989). It has been found to exhibit the lowest root mean square error (RMSE) when compared with several other interpolation methods when the dataset was projected to a UTM (Merwade *et al*., 2006). The quality of the 3D depth surface was evaluated by extracting interpolated depth values at locations where the validation dataset was taken and RMSE analyses conducted. The 3D Analyst Extension tool, ArcScene, raster digital elevation model, and Triangular Irregular Network (TIN) model were utilized to provide a visual 2.5-dimensional perspective (false 3D) of the river bathymetric output in ArcGIS 9.2 (Figure 4).

Figure 4. A false 3D (2.5 dimensional perspective) image of the surveyed section of the Cagayan de Oro River

2.4 Erosion Impact on Sediment Load

With time series river depth profiles, the amount of sediment load increase/decrease over time, as well as the spatial location of erosion and deposition that can be determined. To demonstrate this bed load change determination, the four cross-section profile data from Siringan *et al.* (1998) located between Carmen and Maharlika Bridges were digitized (Figure 5). This profile served as the "before-river-depth". The "after-river-depth" model was extracted from the bathymetric model generated using the spatial extent coordinates of the "before-river-depth" model. The "before" and "after" models were subjected to the cut/fill tool of ArcGIS 9.2 3D Analyst Extension to detect the change.

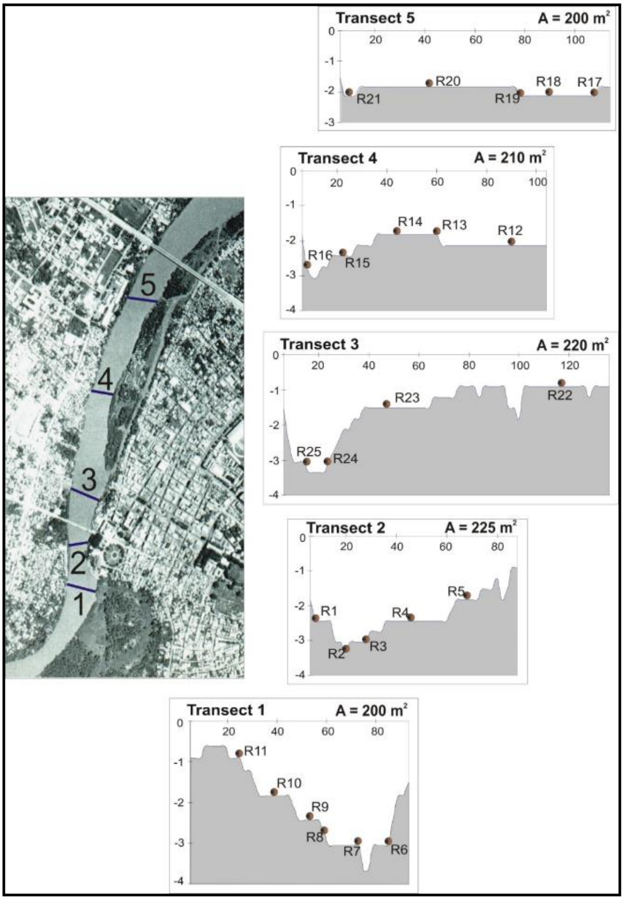

Figure 5. Historical transects with river depth profile of the Cagayan River (Siringan *et al*., 1998)

2.5 Historical River Cross Section Comparison

The four transects used in the erosion impact component of this study were used to document change with river depth over time. Scatterplots were generated with the X-axis representing the width of the river, and the Y-axis representing the depth of the river. Two types of data generated by the study were used to compare with the historical data – the nearest actual data points collected and the interpolated values. Comparison through translation was done by moving the nearest sampled point toward the transect location (Figure 6). The justification of the process of translation was based on an intuitive realization that the flow of the water in one direction creates an anisotropic condition where data points along the flow of the water were more closely correlated with one another compared to data points across the width of the river. The comparison dataset from the interpolated figures was derived from the 3D model of river depth using ArcGIS 9.2 3D analyst. The figures were obtained at the location of the historical transect by using the extract profile function.

Figure 6. Illustration of how actual data points taken during a river depth profile survey using Humminbird echo sounder were translated/moved toward to the location of the transect line to approximate current river depth.

2.6 Flood Area Simulation

To demonstrate spatial flooding as a consequence of water level rise using the data generated by this study, flood scenarios were created using the (Advanced Space-borne Thermal Emission and Reflection Radiometer (ASTER)-derived global digital elevation model (GDEM), the elevation of river surface collected by the Trimble ProXRS GPS, and the JAXA ALOS digitized river edge. With the ASTER GDEM, sample flooded area estimations were generated of scenarios where the Cagayan de Oro River runs its bank at 2, 4 and 6 meters, respectively, above normal. These numbers were based on the visual extent of the flooded areas as observed by the researchers from the field. With the river edge considered as 0 meters, the areal extent when water reaches the 2, 4, and 6 meters were calculated within ArcGIS.

3. Results and Discussion

Table 1 summarizes the relevant statistics on data generated by the equipment used in the study. The ProXRS GPS receiver was set to collect data at 2-second intervals, while the Humminbird was set to collect data at 5-second intervals on the first day. Table 2 summarizes different depth categories, the area covered, and the corresponding proportion of the overall area of the surveyed Cagayan de Oro River, based on the generated 3D depth model.

Table 1. Relevant statistics on the quantity of depth and spatial resolution of data points collected during the survey

Equipment	Day	Mean (m)	Std. Dev.	Min (m)	Max (m)
ProXRS	1	1.73	1.86	0.10	60.53
	2	2.06	2.72	0.10	88.05
Humminbird	1	12.17	11.73	1.76	96.14
	2	12.91	9.96	1.76	87.37

Table 2. Cagayan de Oro river depth profile distribution based on 3 dimensional interpolated surface

Depth (m)	Area (ha)	%
≤1	94.1	50.24
> 1 to 2	51.9	27.75
> 2 to 3	24.4	13.01
> 3 to 4	8.3	4.45
> 4 to 5	3.5	1.90
> 5 to 6	2.0	1.08
> 6 to 8	2.0	1.09
> 8	0.9	0.48
Total	187.3	100.00

A new sandbar was formed at the portion adjacent to Barangay Consolacion (indicated by a red circle on the map in Figure 7a). Quarrying activities of sand were also rampant in the segment between Puntod-Kauswagan Bridge and Carmen Bridge. Visual inspection of the river depth model revealed that in the segment from the Pelaez Bridge to the Maharlika Bridge, most of the areas had depths less than 4 m.

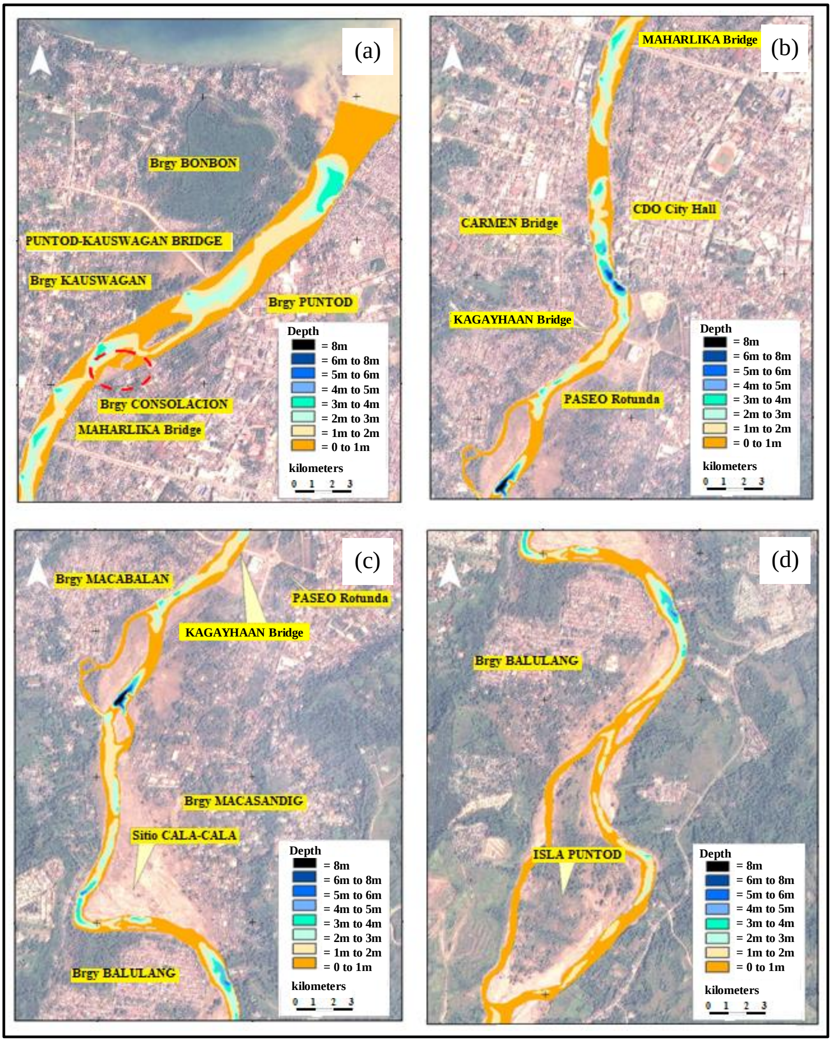

Figure 7. The bathymetry of the Cagayan de Oro river across four sections: Maharlika to Kauswagan (a), Kagayhaan to Carmen to Maharlika bridges (b), Villa Angela, Barangay Balulang to the Kagayhaan Bridge (c) and Villa Angela section to Isla Puntod (d)

There were patches of deep sections with a depth greater than 6 m such as those adjacent to the St. Augustine Metropolitan Cathedral and river section 1.5 km southwest of Paseo del Rio (Figures 7b, 7c). Figure 7d showed shallow to medium depth areas of the river. Deep portions of the river can be found at the section beyond Pelaez Bridge, with a depth more than 8m (Figure 8).

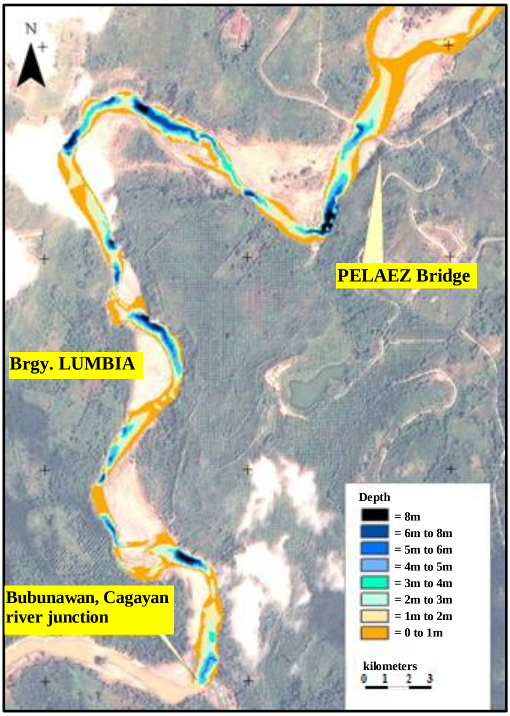

Figure 8. River bathymetry from Bubunawan
to the Pelaez bridge

In terms of area, 78% of the river area is less than 2 m deep. Only 2.66% of the river had the depth of more than 5 m, which was located mostly from Bubunawan-Cagayan de Oro River junction near the Pelaez Bridge. To provide an objective measure of interpolated values fit to actual sonar readings, a subset of 269 (out of 1712 readings) randomly selected readings were used as validation dataset to generate RMSE. Observed RMSE between validation and interpolated values was 1.186 m.

3.1 Equipment Performance

The degree of maneuverability of the designed raft platform was affected by the degree of flowing water turbulence. In areas of the river where the water was deep and moving slowly, a diagonal zigzag path moving from one side of the river to the other was taken. In sections of the river where the river current was relatively fast moving, there was difficulty following a zigzag pattern, although the team tried to meander from one side of the river to the other as much as possible to obtain variations in river depth. Finally, in sections of the river where the water was very turbulent and fast-moving, the team was not in a position to direct the sideward movement of the survey, so depth sensing was confined to where the water current guided the raft. Satellite acquisition was very challenging in areas of the river channel flanked by massive stone cliffs on the left side of the moving raft, at the upper section of the surveyed river before the Pelaez Bridge.

3.2 River Bed Morphology

3.2.1 Erosion Impact on Sediment Load

Figure 9 shows the result of the cut and fill tool in ArcGIS 9.2 showing the before (Siringan *et al*., 1998) and after (data generated by this study) storm impact on sediment load. On the other hand, Figure 10 shows the areas of erosion and deposition, as well as depth change over time (Figure 10a). Using the information contained in the maps, areas to be dredged can be easily determined. In this scenario, for example, the red colored areas need to be dredged (Figure 10b). The volume of sediments eroded and deposited along the segment can also be determined. Table 3 shows that the volume of sediments eroded along the illustration segment was 3.8 times greater than the volume of sediments deposited.

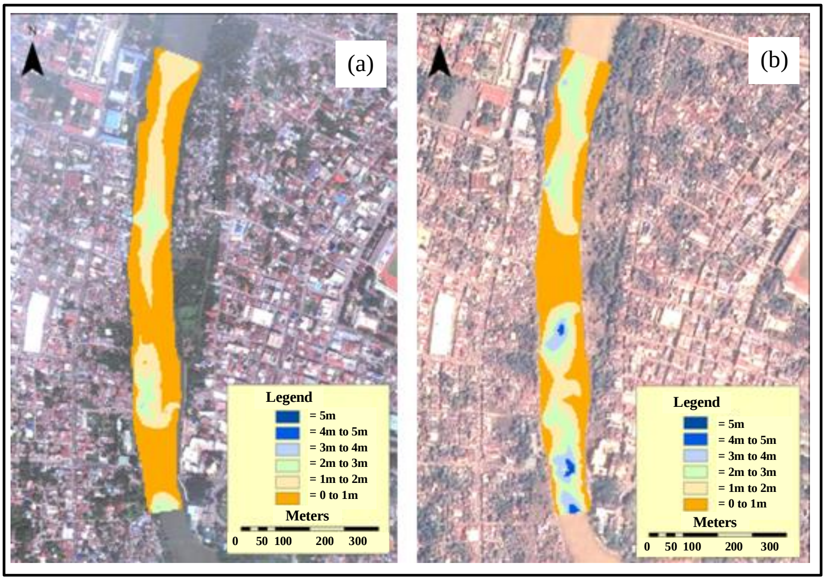

Figure 9. Result of cut and fill analysis (using ArcGIS 9.2) of a section of the Cagayan de Oro River showing Siringan *et al.* (1998) cross section depth profiles (a) and depth derived from the depth points collected by the Humminbird sonar unit (b)

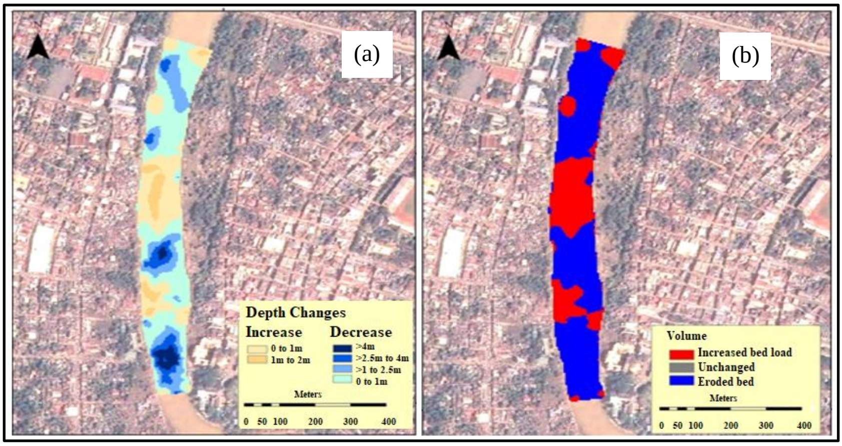

Figure 10. Areas of erosion and deposition along a segment of the Cagayan de Oro River showing depth changes (a) and estimated impact on river bed load (b)

Table 3. Summary of deposited and eroded sediments

	Volume (cu.m.)	Area (ha)
Sediment Deposited	27,890	5.340
Sediment Eroded	106,448	10.565

3.2.2 Historical River Cross Section Comparison

One does not expect the measurement of river profile taken by drawing a perpendicular line across the river channel to be static over time. However, conducting a comparison will still be informative, as it provides an objective way of looking at changes in the river morphology as a result of significant natural calamity events. Figure 11 shows the results of comparing historical data (Siringan *et al*., 1998) with depth values generated through translation and profile extraction using the ArcGIS 9.2 3D analyst. As expected, data coming from the different sources and temporal context did not agree, although the model and translated points were closer to one another, as they were derived from the same dataset. The distance from the transect line of the translated points could be a factor in the observed difference, as well as the reliability of the generated 3D interpolated model. Although it might be justified to attribute the observed changes to be due to the flood event, the coarse distribution of depth data prevented the researchers from giving a definitive conclusion with a high level of certainty. Furthermore, one has to consider the significant amount of time that elapsed since the Siringan *et al.* (1998) data was published. Physically, the interpolated model tends to average large depths at the left bank with the depth of shallower water. The impression was that some parts of the river had become deeper compared to the historical data, while other parts were shallower.

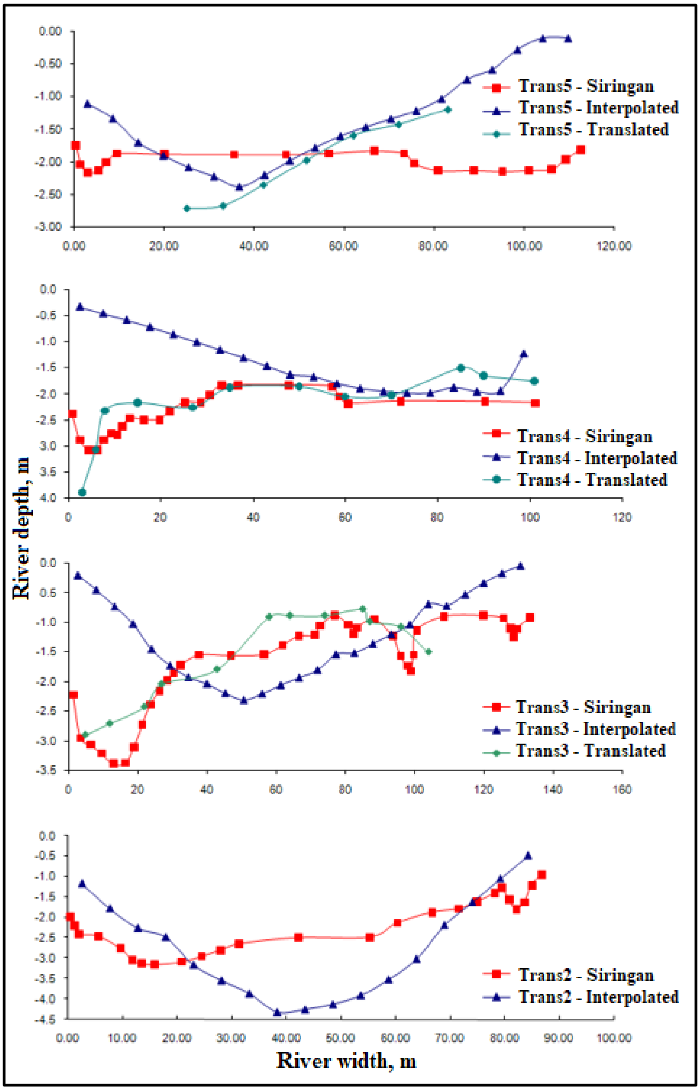

Figure 11. Comparison of depth profile coming from Siringan *et al*. (1998), interpolated and actual values from river depth measurements using Humminbird echo sounder

3.2.3 Flood Simulation Area

Figures 12a, 12b, and 12c show the simulated flood areal coverage when a section of the Cagayan de Oro River rises 2, 4, and 6 meters, respectively – resulting in the flooding of 164, 211 and 245 hectares (inclusive of surface area occupied by the river), respectively. The simulated areal extent of flooding is confined to the boundaries of the identified section of the river as shown in Figure 12.

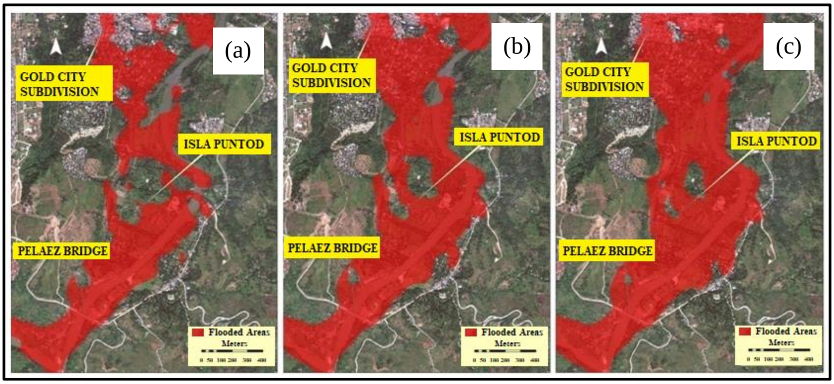

Figure 12. Three flooding scenarios of a section of the Cagayan de Oro River showing impact of increase in water height at 2 m (a), 4 m (b) and 6 m (c) above normal level

4. Conclusion and Recommendation

A raft equipped with echo sounder and a GPS receiver was used to obtain depth readings; relevant secondary data were obtained and processed; and a 3D depth profile of the Cagayan de Oro River was generated. Confidence in the generated 3D bathymetric model of the river was made possible by the use of a calibration technique where an observed error in a non-moving component of the setup over a known point was used to reduce errors in the moving part of the setup through a process known as differential correction. In addition, the observed RMSE of the generated 3D bathymetric model of the river against the validation dataset was 1.186 m. The generated bathymetric data was used to generate sediment net loss and deposition, as well as temporal change analysis and flood modeling. In the future, results obtained in this study can be compared with results from more elaborate methodologies. Furthermore, replication of what has been done in this study can be performed several times over the course of a year or some logical interval of time, or right after every change in the amount and flow pattern of the river. The generated bathymetric models after each instance can provide validation on the usefulness of this study.

5. References

Alfieri, L., Feyen, L., Salamon, P., Thielen, J., Bianchi, A., & Dottori, F. (2016). Modeling the socio-economic impact of river floods in Europe. Natural Hazards and Earth System Sciences, 16(6), 1401-1411.

Buffington, J.M. (2012). Changes in channel morphology over human time scales gravel-bed rivers (pp. 433-463). Hoboken, NJ: John Wiley.

Ceylan, A., & Ekizoglu, I. (2014). Avaliação de mapas batimétricos via SIG para água em reservatório. Boletim de Ciências Geodésicas, 20(1), 142-158. http://dx.doi.org/10.1590/ s1982-21702014000100010.

Department of Environment and Natural Resources (DENR). (2017). Region 10 ENR Profile, 2017. Retrieved from http://r10.denr.gov.ph/images/photo-releases/2018/ October/r10profile_enr_updated102218.pdf_compressed.pdf.

Drakopoulou, P., Kapsimalis, V., Parcharidis, I., & Pavlopoulos, K. (2018). Retrieval of nearshore bathymetry in the Gulf of Chania, NW Crete, Greece, from WorldWiew-2 multispectral imagery. Proceedings of SPIE 10773, Sixth International Conference on Remote Sensing and Geoinformation of the Environment, Paphos, Cyprus. https://doi.org/10.1117/12.2326189

Garcıa-Pintado, J., Mason, D.C., Dance, S.L., Cloke, H.L., Neal, J.C., & Freer, J. (2015). Satellite-supported flood forecasting in river networks: a real case study. Journal of Hydrology, 523, 706-724.

Grimaldi, S., Li, Y., Walker, J.P., & Pauwels, V.R.N. (2018). Effective representation of river geometry in hydraulic flood forecast models. Water Resources Research, 54(6), 1031-1057. https://doi.org/10.1002/2017WR021765

Hilldale, R.C., & Raff, D. (2008). Assessing the ability of airborne LiDAR to map river bathymetry. Earth Surface Processes and Landforms 33(5), 773-783.

Hutchinson, M.F. (1989). A new procedure for gridding elevation and stream line data with automatic removal of spurious pits. Journal of Hydrology, 106, 211-232.

Manila Observatory. (2011). Preliminary analysis on extreme weather event Tropical Storm Sendong. Quezon City, Manila Observatory: 17. Retrieved from https://essc.org.ph/content/view/614/44/. Accessed 2019-07-24.

Merwade, V.M., Maidment, D.R., & Goff, J.A. (2006). Anisotropic considerations while interpolating river channel bathymetry. Journal of Hydrology, 331, 731-741.

Oouchi, K., Yoshimura, J., Yoshimura, H., Mizuta, R., Kusunoki, S., & Noda, A. (2006). Tropical cyclone climatology in a global-warming climate as simulated in a 20 km-mesh global atmospheric model: frequency and wind intensity analyses. Journal of the Meteorological Society of Japan, 84(2), 259-276. doi: 10.2151/jmsj.84.259.

Perez, J.F., Swain, N.R., Dolder, H.G., Christensen, S.D., Snow, A.D., & Nelson, E.J. (2016). From global to local: providing actionable flood forecast information in a cloud-based computing environment. JAWRA Journal of the American Water Resources Association, 52(4), 965-978.

US Department of Defense. (2008). Global Positioning System Standard Positioning Service Performance Standard (4th Eds.). Washington, DC: US Department of Defense.

Shcherbina, A.Y., Gawarkiewicz, G.G., Linder, C.A., & Thorrold, S.R. (2008). Mapping bathymetric and hydrographic features of Glover's Reef, Belize, with a REMUS autonomous underwater vehicle, Limnology and Oceanography, 53(2), 2264-2272. doi: 10.4319/lo.2008.53.5_part_2.2264.

Siringan, F.P., Berdin, R.D., Doruelo, J.S., Jaraula, C.M.B., Mateo, Z.R.P., Ong, J.B., & Yacat, Y.Y. (1998). Sedimentation patterns and sediment dispersal along the coast of Macajalar Bay: establishing environmental baselines and predictive tools for coastal resource management using the sediment record (Terminal Report). Diliman, Quezon City: National Institute of Geological Sciences (NIGS)-University of the Philippines.

Soar, P., Wallerstein, N., & Thorne, C. (2017). Quantifying river channel stability at the basin scale. Water, 9(2), 133.

Traganos, D., Poursanidis, D., Aggarwal, B., Chrysoulakis, N., & Reinartz, P. Estimating satellite-derived bathymetry (SDB) with the google earth engine and sentinel-2. Remote Sensing, 10(6), 859.

Trigg, M.A., Wilson, M.D., Bates, P.D., Horritt, M.S., Alsdorf, D.E., & Forsberg, B. R. (2009). Amazon flood wave hydraulics. Journal of Hydrology, 374(1-2), 92-105.

Wood, M., Hostache, R., Neal, J., Wagener, T., Giustarini, L., & Chini, M. (2016). Calibration of channel depth and friction parameters in the LISFLOOD-FP hydraulic model using medium-resolution SAR data and identifiability techniques. Hydrology and Earth System Sciences, 20(12), 4983-4997.